Project GHZ experiment

Reference 2: "Experimental Test of Quantum Nonlocality in Three-Photon GHZ Entanglement"
From the journal Nature February 2000.

Comments on notation etc.

This paper is a almost a direct copy of the whole problem assigned. There are small notational differences to note in reading this article.

1) They begin with the GHZ state which is slightly different than we have (although note that in reference 1 the GHZ state is the same as ours). They start with |H>|H>|H> + |V>|V>|V>. The difference is only in the phases of the terms you get for the quantum kets. See eqn 4. This should be identical to the state you found in part C2 (the yyx state), except for the phases (they have all plus signs). These phases do not effect the argument of the article.
2) You probably immediately noticed that eqn 4 doesn't agree with yours. If you examine equations 2 and 3, you will see what we call |P> and |M>, they call |H'> and |V'> respectively. Thus whenever you see a H' in the article, think P and V' think M. It all works.
3) There is some stuff on experimental details, you can gloss over these.

A paragraph by paragraph comparison goes as follows:

Paragraph 1: Just states the GHZ state in the zzz basis (HV basis). This you derived in step B1 (though note difference above.

Paragraph 2: This defines the basis as you did problem A. See that they agree.
Paragraph 3: This corresponds to problem C2.
Paragraph 4: Says you can get others (C3, and C4) by permutation. You derived them explicitly.
Paragraph 5: Start real local hidden variable model. Reasoning for instruction sets.
Paragraph 6: Defines what we call parity.
Paragraph 7: Just includes the result from problem C1.

Paragraph 8: Argues what xxx state instruction set should be. This is a different argument than we pursued. This argument states that the instruction set should be the opposite of our xxx ket. What we tried to do is to make our instruction set compatible with the C1,C3, and C4 quantum kets and found that we got differences with the C2 (yyx) result then. A slightly different approach. They argue that (given parity of yyx, yxy, and xyy) the instruction set should have parity –1.

Paragraph 9: States what xxx state is (problem C1 again). States also that these terms do not agree with what the instruction set gives.

Paragraph 10: GHZ only needs 1 measurement (ideally) to discriminate between QM and Classical.

Paragraph 11: Discussion of experimental set up.
Paragraph 12: Differences with older Bell Ineq. Violations experiments.
Paragraph 13: Explains exactly how you observe a violation.
Paragraph 14: Starts to discuss experiment error (details).
Paragraph 15: Possible counter-arguments since measurements are not perfect.

***Paragraph 16:** The results for one possible case (yyx) and what data look like. Figure 3 is what you want to examine. Compare these results (especially the top one) with the ket you obtained in C2 AND your instruction sets (which are opposite. You should find that they agree with your ket and not your set.

Paragraph 17: Explains some experimental error and results. See fig 4. This is based on xxx state as argued in paragraph 8.
Paragraph 18: Discusses the experimental results discussed in previous paragraph.
Paragraph 19: Some details (don't worry).
Paragraph 20: Extensions they would like to do.

electrons could be employed to probe atoms and molecules remotely while minimizing the perturbing influences of a nearby local probe—these unwanted interactions might be chemical in nature or result from electric or magnetic fields emanating from an STM tip or other probe device. Our results also suggest altered geometries such as ellipsoids confining bulk electrons, or specially shaped electron mirrors (such as parabolic reflectors) electronically coupling two or more points. One might additionally envision performing other types of 'spectroscopy-at-a-distance' beyond electronic structure measurements, for example, detecting vibrational[16] or magnetic excitations.

We conclude with some remaining questions. Our calculations show that ellipses have a class of eigenmodes that possess strongly peaked probability amplitude near the classical foci (Fig. 3e and f are good examples). Our experiments reveal that the strongest mirages occur when one of these eigenmodes is at E_F and therefore at the energy of the Kondo resonance. When perturbed by a focal atom, this eigenmode still has substantial density surrounding both foci; it is therefore plausible that this quantum state 'samples' the Kondo resonance on the real atom and transmits that signal to the other focus. The physics behind this process is not completely understood. Also, given that a Kondo signature is detected at the empty focus, does this imply that a measurement there is simply providing us with a remote probe of the Co atom with the intervening two-dimensional electrons acting essentially like a wire? Or, as the Kondo effect on the Co atom requires a net spin polarization of the surrounding electron gas, does the projection of the Kondo resonance imply a modified spin polarization at the empty focus? We speculate that both interpretations are actually correct. Full answers to these questions, however, await further experimental and theoretical efforts.

Received 12 October; accepted 14 December 1999.

1. Spector, J., Stormer, H. L., Baldwin, K. W., Pfeiffer, L. N. & West, K. W. Electron focusing in two-dimensional systems by means of an electrostatic lens. *Appl. Phys. Lett.* **56,** 1290–1292 (1990).
2. Crommie, M. F., Lutz, C. P. & Eigler, D. M. Confinement of electrons to quantum corrals on a metal surface. *Science* **262,** 218–220 (1993).
3. Heremans, J. J., von Molnár, S., Awschalom, D. D. & Gossard, A. C. Ballistic electron focusing by elliptic reflecting barriers. *Appl. Phys. Lett.* **74,** 1281–1283 (1999).
4. Kondo, J. Resistance minimum in dilute magnetic alloys. *Prog. Theor. Phys.* **32,** 37–49 (1964).
5. Li, J., Schneider, W.-D., Berndt, R. & Delley, B. Kondo scattering observed at a single magnetic impurity. *Phys. Rev. Lett.* **80,** 2893–2896 (1998).
6. Madhavan, V., Chen, W., Jamneala, T., Crommie, M. F. & Wingreen, N. S. Tunnelling into a single magnetic atom: Spectroscopic evidence of the Kondo resonance. *Science* **280,** 567–569 (1998).
7. Kittel, C. *Quantum Theory of Solids* (Wiley, New York, 1963).
8. Hewson, A. C. *The Kondo Problem to Heavy Fermions* (Cambridge Univ. Press, Cambridge, 1997).
9. Fano, U. Effects of configuration interaction on intensities and phase shifts. *Phys. Rev.* **124,** 1866–1878 (1961).
10. Crommie, M. F., Lutz, C. P. & Eigler, D. M. Imaging standing waves in a two-dimensional electron gas. *Nature* **363,** 524–527 (1993).
11. Hasegawa, Y. & Avouris, P. Direct observation of standing wave formation at surface steps using scanning tunneling spectroscopy. *Phys. Rev. Lett.* **71,** 1071–1074 (1993).
12. Eigler, D. M. & Schweizer, E. K. Positioning single atoms with a scanning tunnelling microscope. *Nature* **344,** 524–526 (1990).
13. Stroscio, J. A. & Eigler, D. M. Atomic and molecular manipulation with the scanning tunneling microscope. *Science* **254,** 1319–1326 (1991).
14. Tomsovic, S. & Heller, E. J. Semiclassical construction of chaotic eigenstates. *Phys. Rev. Lett.* **70,** 1405–1408 (1993).
15. Chan, Y. S. & Heller, E. J. Scanning tunnel microscopy surface state electron scattering: Two-tip results from one-tip data. *Phys. Rev. Lett.* **78,** 2570–2572 (1997).
16. Stipe, B. C., Rezaei, M. A. & Ho, W. Single-molecule vibrational spectroscopy and microscopy. *Science* **280,** 1732–1735 (1998).
17. Lang, N. D. Spectroscopy of single atoms in the scanning tunneling microscope. *Phys. Rev. B* **34,** 5947–5950 (1986).
18. Everson, M. P., Jaklevic, R. C. & Shen, W. Measurement of the local density of states on a metal surface: Scanning tunneling spectroscopic imaging of Au(111). *J. Vac. Sci. Technol. A* **8,** 3662–3665 (1990).
19. Kittel, C. Indirect exchange interactions in metals. *Solid State Phys.* **22,** 1–26 (1968).

Acknowledgements

We thank B. A. Jones, E. J. Heller, J. S. Hersch, G. Fiete, A. J. Heinrich and C. T. Rettner for helpful discussions, and L. Folks for expert assistance with image preparation.

Correspondence and requests for materials should be addressed to H.C.M. (e-mail: hari@alumni.princeton.edu).

Experimental test of quantum nonlocality in three-photon Greenberger–Horne–Zeilinger entanglement

Jian-Wei Pan*, Dik Bouwmeester†, Matthew Daniell*, Harald Weinfurter‡ & Anton Zeilinger*

* *Institut für Experimentalphysik, Universität Wien, Boltzmanngasse 5, 1090 Wien, Austria*
† *Clarendon Laboratory, University of Oxford, Parks Road, Oxford OX1 3PU, UK*
‡ *Sektion Physik, Ludwig-Maximilians-Universität of München, Schellingstrasse 4/III, D-80799 München, Germany*

Bell's theorem[1] states that certain statistical correlations predicted by quantum physics for measurements on two-particle systems cannot be understood within a realistic picture based on local properties of each individual particle—even if the two particles are separated by large distances. Einstein, Podolsky and Rosen first recognized[2] the fundamental significance of these quantum correlations (termed 'entanglement' by Schrödinger[3]) and the

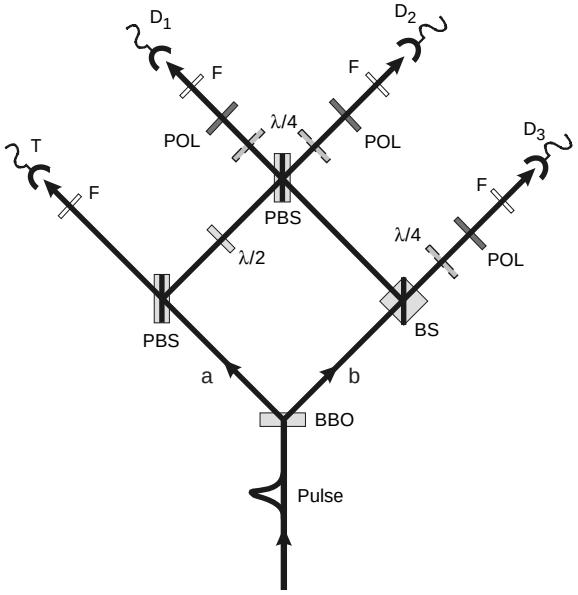


Figure 1 Experimental set-up for Greenberger–Horne–Zeilinger (GHZ) tests of quantum nonlocality. Pairs of polarization-entangled photons[28] (one photon *H* polarized and the other *V*) are generated by a short pulse of ultraviolet light (~ 200 fs, λ = 394 nm). Observation of the desired GHZ correlations requires fourfold coincidence and therefore two pairs[29]. The photon registered at T is always *H* and thus its partner in **b** must be *V*. The photon reflected at the polarizing beam-splitter (PBS) in arm **a** is always *V*, being turned into equal superposition of *V* and *H* by the λ/2 plate, and its partner in arm **b** must be *H*. Thus if all four detectors register at the same time, the two photons in D_1 and D_2 must either both have been *VV* and reflected by the last PBS or *HH* and transmitted. The photon at D_3 was therefore *H* or *V*, respectively. Both possibilities are made indistinguishable by having equal path lengths via **a** and **b** to D_1 (D_2) and by using narrow bandwidth filters ($F \approx 4$ nm) to stretch the coherence time to about 500 fs, substantially larger than the pulse length[30]. This effectively erases the prior correlation information and, owing to indistinguishability, the three photons registered at D_1, D_2 and D_3 exhibit the desired GHZ correlations predicted by the state of equation (1), where for simplicity we assume the polarizations at D_3 to be defined at right angles relative to the others. Polarizers oriented at 45° and λ/4 plates in front of the detectors allow measurement of linear *H′*/*V′* (circular *R*/*L*) polarization.

© 2000 Macmillan Magazines Ltd

two-particle quantum predictions have found ever-increasing experimental support[4]. A more striking conflict between quantum mechanical and local realistic predictions (for perfect correlations) has been discovered[5,6]; but experimental verification has been difficult, as it requires entanglement between at least three particles. Here we report experimental confirmation of this conflict, using our recently developed method[7] to observe three-photon entanglement, or 'Greenberger–Horne–Zeilinger' (GHZ) states. The results of three specific experiments, involving measurements of polarization correlations between three photons, lead to predictions for a fourth experiment; quantum physical predictions are mutually contradictory with expectations based on local realism. We find the results of the fourth experiment to be in agreement with the quantum prediction and in striking conflict with local realism.

We first analyse certain quantum predictions for the entangled three-photon GHZ state:

$$|\Psi\rangle = \frac{1}{\sqrt{2}}(|H\rangle_1|H\rangle_2|H\rangle_3 + |V\rangle_1|V\rangle_2|V\rangle_3) \quad (1)$$

where H and V denote horizontal and vertical linear polarizations respectively. This state indicates that the three photons are in a quantum superposition of the state $|H\rangle_1|H\rangle_2|H\rangle_3$ (all three are horizontally polarized) and the state $|V\rangle_1|V\rangle_2|V\rangle_3$ (all three are vertically polarized) with none of the photons having a well-defined state on its own.

We consider now measurements of linear polarization along directions H'/V' rotated by 45° with respect to the original H/V directions, or of circular polarization L/R (left-handed, right-handed). These new polarizations can be expressed in terms of the original ones as:

$$|H'\rangle = \frac{1}{\sqrt{2}}(|H\rangle + |V\rangle)$$
$$|V'\rangle = \frac{1}{\sqrt{2}}(|H\rangle - |V\rangle) \quad (2)$$

$$|R\rangle = \frac{1}{\sqrt{2}}(|H\rangle + i|V\rangle)$$
$$|L\rangle = \frac{1}{\sqrt{2}}(|H\rangle - i|V\rangle) \quad (3)$$

For convenience we will refer to a measurement of H'/V' linear polarization as an x measurement and one of R/L circular polarization as a y measurement.

Representing the GHZ state (equation (1)) in the new states by using equations (2) and (3), one obtains the quantum predictions for measurements of these new polarizations. For example, for the case of measurement of circular polarization on, say, both photon 1 and 2, and linear polarization H'/V' on photon 3, denoted as a *yyx* experiment, the state may be expressed as:

$$|\Psi\rangle = \frac{1}{2}(|R\rangle_1|L\rangle_2|H'\rangle_3 + |L\rangle_1|R\rangle_2|H'\rangle_3 + |R\rangle_1|R\rangle_2|V'\rangle_3 + |L\rangle_1|L\rangle_2|V'\rangle_3) \quad (4)$$

This expression implies, first, that any specific result obtained in any individual or in any two-photon joint measurement is maximally random. For example, photon 1 will exhibit polarization R or L with the same probability of 50%, or photons 1 and 2 will exhibit polarizations *RL*, *LR*, *RR* or *LL* with the same probability of 25%. Second, given any two results of measurements on any two photons, we can predict with certainty the result of the corresponding measurement performed on the third photon. For example, suppose photons 1 and 2 both exhibit right-handed R circular polarization. Then by the third term in equation (4), photon 3 will definitely be V' polarized.

By cyclic permutation, we can obtain analogous expressions for any experiment measuring circular polarization on two photons and H'/V' linear polarization on the remaining one. Thus, in every one of the three *yyx*, *yxy*, and *xyy* experiments, any individual measurement result—both for circular polarization and for linear H'/V' polarization—can be predicted with certainty for every photon given the corresponding measurement results of the other two.

Now we will analyse the implications for local realism. As these predictions are independent both of the spatial separation and of the relative time order of the three measurements, we consider them performed simultaneously in a given reference frame—say, for conceptual simplicity, in the reference frame of the source. Then, as Einstein locality implies that no information can travel faster than the speed of light, this requires any specific measurement result obtained for any photon never to depend on which specific measurements are performed simultaneously on the other two nor on their outcome. The only way then for local realism to

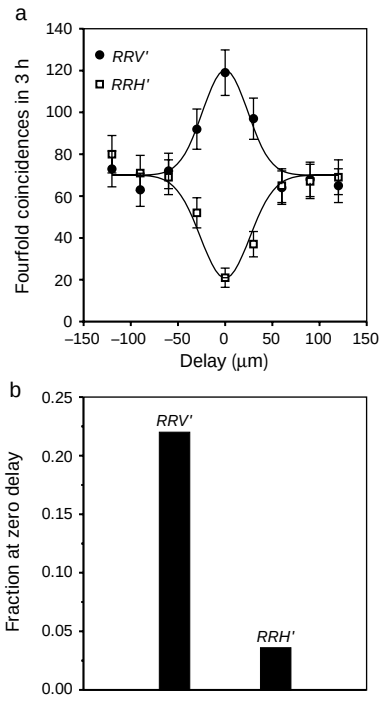


Figure 2 A typical experimental result used in the GHZ argument. This is the *yyx* experiment measuring circular polarization on photons 1 and 2 and linear polarization on the third. **a**, Fourfold coincidences between the trigger detector T, detectors D_1 and D_2 (both set to measure a right-handed polarized photon), and detector D_3 (set to measure a linearly polarized H' (lower curve) and V' (upper curve) photon as a function of the delay between photon 1 and 2 at the final polarizing beam-splitter). We could adjust the time delay between paths **a** and **b** in Fig. 1 by translating the final polarizing beam-splitter (PBS) and using additional mirrors (not shown in Fig. 1) to ensure overlap of both beams, independent of mirror displacement. At large delay, that is, outside the region of coherent superposition, the two possibilities *HHH* and *VVV* are distinguishable and no entanglement results. In agreement with this explanation, it was observed within the experimental accuracy that for large delay the eight possible outcomes in the *yyx* experiment (and also the other experiments) have the same coincidence rate, whose mean value was chosen as a normalization standard. **b**, At zero delay maximum GHZ entanglement results; the experimentally determined fractions of *RRV′* and *RRH′* triples (out of the eight possible outcomes in the *yyx* experiment) are deduced from the measurements at zero delay. The fractions were obtained by dividing the normalized fourfold coincidences of a specific outcome by the sum of all possible outcomes in each experiment—here, the *yyx* experiment.

© 2000 Macmillan Magazines Ltd

explain the perfect correlations predicted by equation (4) is to assume that each photon carries elements of reality for both x and y measurements that determine the specific individual measurement result[5,6,8].

For photon i we call these elements of reality X_i with values +1(−1) for $H'(V')$ polarizations and Y_i with values +1(−1) for $R(L)$; we thus obtain the relations[8] $Y_1Y_2X_3 = -1$, $Y_1X_2Y_3 = -1$ and $X_1Y_2Y_3 = -1$, in order to be able to reproduce the quantum predictions of equation (4) and its permutations.

We now consider a fourth experiment measuring linear H'/V' polarization on all three photons, that is, an *xxx* experiment. We investigate the possible outcomes that will be predicted by local realism based on the elements of reality introduced to explain the earlier *yyx*, *yxy* and *xyy* experiments.

Because of Einstein locality any specific measurement for x must be independent of whether an x or y measurement is performed on the other photon. As $Y_iY_i = +1$, we can write $X_1X_2X_3 = (X_1Y_2Y_3)(Y_1X_2Y_3)(Y_1Y_2X_3)$ and obtain $X_1X_2X_3 = -1$. Thus from a local realist point of view the only possible results for an *xxx* experiment are $V'V'V'$, $H'H'V'$, $H'V'H'$, and $V'H'H'$.

How do these predictions of local realism for an *xxx* experiment compare with those of quantum mechanics? If we express the state given in equation (1) in terms of H'/V' polarization using equation (2) we obtain:

$$|\Psi\rangle = \frac{1}{2}(|H'\rangle_1|H'\rangle_2|H'\rangle_3 + |H'\rangle_1|V'\rangle_2|V'\rangle_3 + |V'\rangle_1|H'\rangle_2|V'\rangle_3 + |V'\rangle_1|V'\rangle_2|H'\rangle_3 \quad (5)$$

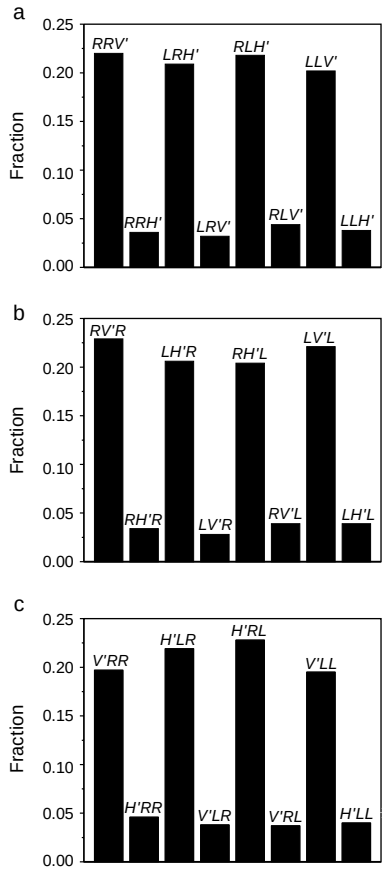


Figure 3 All outcomes observed in the *yyx*, *yxy* and *xyy* experiments, obtained as in Fig. 2. **a**, *yyx*; **b**, *yxy*; **c**, *xyy*. The experimental data show that we observe the GHZ terms predicted by quantum physics (tall bars) in a fraction of 0.85 ± 0.04 of all cases and 0.15 ± 0.02 of the spurious events (short bars) in a fraction of all cases. Within our experimental error we thus confirm the GHZ predictions for the experiments.

Thus we conclude that the local realistic model predicts none of the terms occurring in the quantum prediction and vice versa. This means that whenever local realism predicts that a specific result will definitely occur for a measurement on one of the photons based on the results for the other two, quantum physics definitely predicts the opposite result. For example, if two photons are both found to be H' polarized, local realism predicts the third photon to carry polarization V' while quantum physics predicts H'. This is the GHZ contradiction between local realism and quantum physics.

In the case of Bell's inequalities for two photons, the conflict between local realism and quantum physics arises for statistical predictions of the theory; but for three entangled particles the conflict arises even for the definite predictions. Statistics now only results from the inevitable experimental limitations occurring in any and every experiment, even in classical physics.

A diagram of our experimental set-up is given in Fig. 1. The method to produce GHZ entanglement for three spatially separated photons is a further development of the techniques that have been used in our previous experiments on quantum teleportation[9] and entanglement swapping[10]. GHZ entanglement has also been inferred for nuclear spins within single molecules from NMR measurements[11], though there a test of nonlocality is impossible.

In the experiment GHZ entanglement is observed under the condition that the trigger detector T and the three GHZ detectors D_1, D_2 and D_3 all actually register a photon. As there are other detection events where fewer detectors fire, this condition might raise doubts about whether such a source can be used to test local realism. The same question arose earlier for certain experiments involving photon pairs[12,13] where a violation of Bell's inequality was only achieved under the condition that both detectors used register a photon. It was often believed[14,15] that such experiments could never, not even in their idealized versions, be genuine tests of local realism. However, this has been disproved[16]. Following the same line of reasoning, it has recently been shown[17] that our procedure permits a valid GHZ test of local realism. In essence, both the Bell and the GHZ arguments exhibit a conflict between detection events and the ideas of local realism.

As explained above, demonstration of the conflict between local realism and quantum mechanics for GHZ entanglement consists of four experiments, each with three spatially separated polarization measurements. First, we perform *yyx*, *yxy* and *xyy* experiments. If the results obtained are in agreement with the predictions for a GHZ state, then for an *xxx* experiment, our consequent expectations using a local-realist theory are exactly the opposite of our expectations using quantum physics.

For each experiment we have eight possible outcomes of which ideally four should never occur. Obviously, no experiment either in classical physics or in quantum mechanics can ever be perfect; therefore, even the outcomes which should not occur will occur with some small probability in any real experiment. The question is how to deal with such spurious events in view of the fact that the original GHZ argument is based on perfect correlations.

We follow two independent possible strategies. In the first strategy we simply compare our experimental results with the predictions both of quantum mechanics and of a local realist theory for GHZ correlations, and assume that the spurious events are attributable to experimental imperfection that is not correlated to the elements of reality a photon carries. A local realist might argue against that approach and suggest that the non-perfect detection events indicate that the GHZ argument is inapplicable. In our second strategy we therefore accommodate local-realist theories, by assuming that the non-perfect events in the first three experiments indicate a set of elements of reality which are in conflict with quantum mechanics. We then compare the local realist prediction for the *xxx* experiment obtained under that assumption with the experimental results.

The observed results for two possible outcomes in a *yyx* experiment

© 2000 Macmillan Magazines Ltd

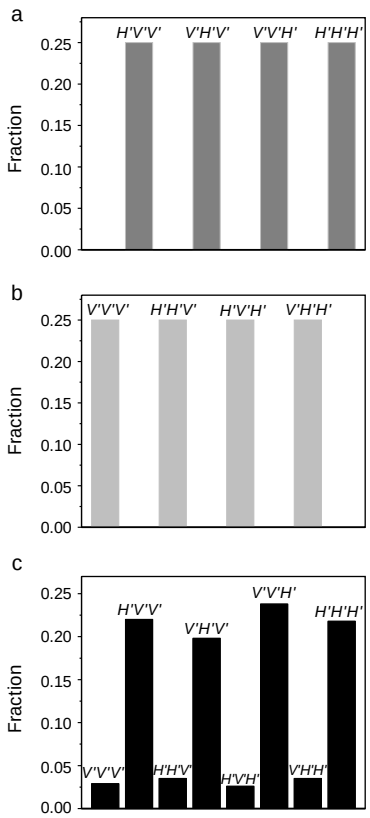


Figure 4 Predictions of quantum mechanics and of local realism, and observed results for the *xxx* experiment. **a, b,**The maximum possible conflict arises between the predictions for quantum mechanics (**a**) and local realism (**b**) because the predicted correlations are exactly opposite. **c,** The experimental results clearly confirm the quantum predictions within experimental error and are in conflict with local realism.

are shown in Fig. 2. The six remaining possible outcomes of a *yyx* experiment have also been measured in the same way and likewise in the *yxy* and *xyy* experiments. For all three experiments this results in 24 possible outcomes whose individual fractions thus obtained are shown in Fig. 3.

Adopting our first strategy, we assume that the spurious events are attributable to unavoidable experimental errors; within the experimental accuracy, we conclude that the desired correlations in these experiments confirm the quantum predictions for GHZ entanglement. Thus we compare the predictions of quantum mechanics and local realism with the results of an *xxx* experiment (Fig. 4) and we observe that, again within experimental error, the triple coincidences predicted by quantum mechanics occur and not those predicted by local realism. In this sense, we believe that we have experimentally realized the first three-particle test of local realism following the GHZ argument.

We then investigated whether local realism could reproduce the *xxx* experimental results shown in Fig. 4c, if we assume that the spurious non-GHZ events in the other three experiments (Fig. 3) actually indicate a deviation from quantum physics. To answer this we adopt our second strategy and consider the best prediction a local realistic theory could obtain using these spurious terms. How, for example, could a local realist obtain the quantum prediction $H'H'H'$? One possibility is to assume that triple events producing $H'H'H'$ would be described by a specific set of local hidden variables such that they would give events that are in agreement with quantum theory in both an *xyy* and a *yxy* experiment (for example, the results $H'LR$ and $LH'R$), but give a spurious event for a *yyx* experiment (in this case, LLH'). In this way any local realistic prediction for an event predicted by quantum theory in our *xxx* experiment will use at least one spurious event in the earlier measurements together with two correct ones. Therefore, the fraction of correct events in the *xxx* experiment can at most be equal to the sum of the fractions of all spurious events in the *yyx*, *yxy*, and *xyy* experiments, that is, 0.45 ± 0.03. However, we experimentally observed such terms with a fraction of 0.87 ± 0.04 (Fig. 4c), which violates the local realistic expectation by more than eight standard deviations.

Our latter argument is equivalent to adopting an inequality of the kind first proposed by Mermin[18]. This second analysis succeeds because our average visibility of 71% ± 4% clearly surpasses the minimum of 50% necessary for a violation of local realism[18–20]. However, we realise that, as for all existing two-particle tests of local realism, our experiment has rather low detection efficiencies. Therefore we had to invoke the fair sampling hypothesis[21,22], where it is assumed that the registered events are a faithful representative of the whole.

Possible future experiments could include: further study GHZ correlations over large distances with space-like separated randomly switched measurements[23]; extending the techniques used here to the observation of multi-photon entanglement[24]; observation of GHZ-correlations in massive objects like atoms[25]; and investigation of possible applications in quantum computation and quantum communication protocols[26,27]. □

1. Bell, J. S. On the Einstein-Podolsky-Rosen paradox. *Physics* **1,** 195–200 (1964); reprinted Bell, J. S. *Speakable and Unspeakable in Quantum Mechanics* (Cambridge Univ. Press, Cambridge, 1987).
2. Einstein, A., Podolsky, B. & Rosen, N. Can quantum-mechanical description of physical reality be considered complete? *Phys. Rev.* **47,** 777–780 (1935).
3. Schrödinger, E. Die gegenwärtige Situation in der Quantenmechanik. *Naturwissenschaften* **23,** 807–812; 823–828; 844–849 (1935).
4. Aspect, A. Bell's inequality test: more ideal than ever. *Nature* **390,** 189–190 (1999).
5. Greenberger, D. M., Horne, M. A. & Zeilinger, A. in *Bell's Theorem, Quantum Theory, and Conceptions of the Universe* (ed. Kafatos, M.) 73–76 (Kluwer Academic, Dordrecht, 1989).
6. Greenberger, D. M., Horne, M. A., Shimony, A. & Zeilinger, A. Bell's theorem without inequalities. *Am. J. Phys.* **58,** 1131–1143 (1990).
7. Bouwmeester, D., Pan, J.-W., Daniell, M., Weinfurter, H. & Zeilinger, A. Observation of three-photon Greenberger-Horne-Zeilinger entanglement. *Phys. Rev. Lett.* **82,** 1345–1349 (1999).
8. Mermin, N. D. What's wrong with these elements of reality? *Phys. Today* **43,** 9–11 (1990).
9. Bouwmeester, D. *et al.* Experimental quantum teleportation. *Nature* **390,** 575–579 (1997).
10. Pan, J.-W., Bouwmeester, D., Weinfurter, H. & Zeilinger, A. Experimental entanglement swapping: Entangling photons that never interacted. *Phys. Rev. Lett.* **80,** 3891–3894 (1998).
11. Laflamme, R., Knill, E., Zurek, W. H., Catasti, P. & Mariappan, S. V. S. NMR Greenberger-Horne-Zeilinger states. *Phil. Trans. R. Soc. Lond. A* **356,** 1941–1947 (1998).
12. Ou, Z.Y. & Mandel, L. Violation of Bell's inequality and classical probability in a two-photon correlation experiment. *Phys. Rev. Lett.* **61,** 50–53 (1988).
13. Shih, Y. H. & Alley, C. O. New type of Einstein-Podolsky-Rosen-Bohm experiment using pairs of light quanta produced by optical parametric down conversion. *Phys. Rev. Lett.* **61,** 2921–2924 (1988).
14. Kwiat, P., Eberhard, P. E., Steinberger, A. M. & Chiao, R. Y. Proposal for a loophole-free Bell inequality experiment. *Phys. Rev. A* **49,** 3209–3220 (1994).
15. De Caro, L. & Garuccio, A. Reliability of Bell-inequality measurements using polarization correlations in parametric-down-conversion photons. *Phys. Rev. A* **50,** R2803–R2805 (1994).
16. Popescu, S., Hardy, L. & Zukowski, M. Revisiting Bell's theorem for a class of down-conversion experiments. *Phys. Rev. A* **56,** R4353–4357 (1997).
17. Zukowski, M. Violations of local realism in multiphoton interference experiments. *Phys. Rev. A* **61,** 022109 (2000).
18. Mermin, N. D. Extreme quantum entanglement in a superposition of macroscopically distinct states. *Phys. Rev. Lett.* **65,** 1838–1841 (1990).
19. Roy, S. M. & Singh, V. Tests of signal locality and Einstein-Bell locality for multiparticle systems. *Phys. Rev. Lett.* **67,** 2761–2764 (1991).
20. Zukowski, M. & Kaszlikowski, D. Critical visibility for *N*-particle Greenberger-Horne-Zeilinger correlations to violate local realism. *Phys. Rev. A* **56,** R1682–1685 (1997).
21. Pearle, P. Hidden-variable example based upon data rejection. *Phys. Rev. D* **2,** 1418–1425 (1970).
22. Clauser, J. & Shimony, A. Bell's theorem: experimental tests and implications. *Rep. Prog. Phys.* **41,** 1881–1927 (1978).
23. Weihs, G., Jennewein, T., Simon, C., Weinfurter, H. & Zeilinger, A. Violation of Bell's inequality under strict Einstein locality conditions. *Phys. Rev. Lett.* **81,** 5039–5043 (1998).
24. Bose, S., Vedral, V. & Knight, P. L. Multiparticle generalization of entanglement swapping. *Phys. Rev. A* **57,** 822–829 (1998).
25. Haroche, S. Atoms and photons in high-Q cavities: next tests of quantum theory. *Ann. NY Acad. Sci.* **755,** 73–86, (1995).
26. Briegel, H.-J., Duer, W., Cirac, J. I. & Zoller, P. Quantum repeaters: The role of imperfect local operations in quantum communication. *Phys. Rev. Lett.* **81,** 5932–5935 (1998).
27. Cleve, R. & Buhrman, H. Substituting quantum entanglement for communication. *Phys. Rev. A* **56,** 1201–1204 (1997).
28. Kwiat, P. G. *et al.* New high intensity source of polarization-entangled photon pairs. *Phys. Rev. Lett.* **75,** 4337–4341 (1995).

© 2000 Macmillan Magazines Ltd

29. Zeilinger, A., Horne, M. A., Weinfurter, H. & Zukowski, M. Three particle entanglements from two entangled pairs. *Phys. Rev. Lett.* **78,** 3031–3034 (1997).
30. Zukowski, M., Zeilinger, A. & Weinfurter, H. Entangling photons radiated by independent pulsed source. *Ann. NY Acad. Sci.* **755,** 91–102 (1995).

Acknowledgements

We thank D. M. Greenberger, M. A. Horne and M. Zukowski for useful discussions. This work was supported by the Austrian Fonds zur Förderung der Wissenschaftlichen Forschung, the Austrian Academy of Sciences and the Training and Mobility of Researchers programme of the European Union.

Correspondence and requests for materials should be addressed to A.Z. (e-mail: Zeilinger-office@exp.univie.ac.at).

Ball lightning caused by oxidation of nanoparticle networks from normal lightning strikes on soil

John Abrahamson & James Dinniss

Chemical and Process Engineering Department, University of Canterbury, Private Bag 4800, Christchurch, New Zealand

Observations of ball lightning have been reported for centuries, but the origin of this phenomenon remains an enigma. The 'average' ball lightning appears as a sphere with a diameter of 300 mm, a lifetime of about 10 s, and a luminosity similar to a 100-W lamp[1]. It floats freely in the air, and ends either in an explosion, or by simply fading from view. It almost invariably occurs during stormy weather[2,3]. Several energy sources have been proposed[2–4] to explain the light, but none of these models has succeeded in explaining all of the observed characteristics. Here we report a model that potentially accounts for all of those properties, and which has some experimental support. When normal lightning strikes soil, chemical energy is stored in nanoparticles of Si, SiO or SiC, which are ejected into the air as a filamentary network. As the particles are slowly oxidized in air, the stored energy is released as heat and light. We investigated this basic process by exposing soil samples to a lightning-like discharge, which produced chain aggregates of nanoparticles: these particles oxidize at a rate appropriate for explaining the lifetime of ball lightning.

Away from buildings, the material most commonly in the path of a lightning strike is a tree, and then soil. Lightning leaves solid tubular or lumpy residues (fulgurites) after interacting with sand or soil, which indicate that the discharge has penetrated beneath the ground surface, and that the material has been molten. If soils or tree roots are regarded as a fine mixture of silica and carbon, then under such high-temperature treatment, one expects chemical reduction to silicon metal, silicon monoxide, or silicon carbide, followed by oxidation by oxygen from the air.

Such reduction of a C/SiO_2 mix using an electric arc is commonly used in industry. Liquid silicon is the dominant equilibrium condensed phase around 3,000 K (ref. 5) for C/SiO_2 mole ratios of 1–2, with solid SiC expected for ratios >2. This ratio can range from 0.1 to about 2 for mineral soils, and is much higher for wood. Silicon metal has been observed[6] in the silicate glass deposit adjacent to a charred tree root after a large lightning strike.

Such fast-cooling processes often yield nanometre-sized particles[7,8]. For lightning action on a soil, or a soil/wood mix with a C/SiO_2 ratio of 1–2, we expect the particles to be Si and SiO (formed by condensation of the dominant vapour species[5]), with SiC and soot dominating for $C/SiO_2 > 2$. Most nanoparticle suspensions are found in the form of chain aggregates[9], which extend where charged particles influence their neighbours[10] (in conditions of higher particle charge and numbers, and fewer gaseous ions, as at cooler flame temperatures). Charge on the growing chain may induce a dendrimer-like structure, growing from the centre. The possible size is suggested by the following observations in quiescent air. Filamentary particle structures spanning 50 mm have been found[11] after vaporizing metal in air in the presence of electric fields. Early work with charged aerosols[12] showed the formation of a spherical networked aerosol suspension of diameter 200 mm.

Particle networks have been proposed more recently[13] as a general basis for ball lightning, with the aggregation influenced by the field of the growing ball[1], but without a clear proposal for the chemical reaction occurring. Oxidation of copper particles has also been suggested[14], but with this process occurring at the perimeter of the sphere of air carrying the particles: a network structure or rate limitation at the particle surface was not mentioned.

A Si/SiO/SiC nanoparticle network would have a large surface, and could be expected to oxidize rapidly, even explosively. However, we emphasize that the rate of oxidation would be limited by the need for oxygen to diffuse through the developing SiO_2 layer to the metal (or carbide) beneath. Laboratory oxidation studies on silicon surfaces[15,16] show that both oxygen and water are reactants. Whether oxygen or water dominate the reaction with silicon depends on their partial pressures. SiC oxidizes at a similar rate to Si (ref. 17).

We checked for the existence of nanosphere chains after exposing soil to a lightning-like discharge. A 10–20 kV d.c. discharge penetrated a 3-mm layer of soil, transferring up to 3.4 C of charge. Sampling of the air space close to the discharge caused deposits to form on a glass-fibre filter and a filter-mounted transmission electron microscope (TEM) grid. Examination of these deposits using scanning electron microscopy (SEM) showed 'lumpy' filament links (width 100 nm, length 10 μm) between the glass fibres. TEM at high resolution (Fig. 1) showed chain aggregates of nanospheres, 5–70 nm in diameter. Larger spheres, several micrometres in diameter, were collected on all the filters, and were collectively of similar mass to the nanoparticles.

Despite using charge transfer within the range observed for lightning strikes[18], we did not observe any luminous ball. At the higher power levels, the soil sample was always completely blown away in the radial direction. It appeared unlikely that a network of delicate long filaments could survive the discharge shockwave. If the

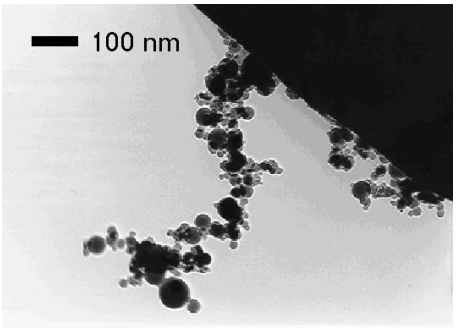


Figure 1 Transmission electron micrograph of nanoparticle chains sampled from the discharge environment. These particles were deposited on a nickel grid, after sampling the gas space above a 14.9-kV discharge on a silt loam soil containing 12.5% carbon. The soil was placed in a layer on a flat conducting (graphite) base below a vertical graphite electrode, with a gap of 22 mm to the soil, and 3.0 C charge transferred from a 204 μF capacitor. The extended chains are made up of spheres 5–70 nm in diameter; the chain width is 25–125 nm. Six of the highest-power runs were examined in this way, with three soils. All showed similar results, except one showing only larger particles.

© 2000 Macmillan Magazines Ltd